

# Universal bottleneck for thermal relaxation in disordered metallic films

*E. M. Baeva<sup>×,+</sup>, N. A. Titova<sup>+</sup>, A. I. Kardakova<sup>+,\*</sup>, S. U. Piatrusha<sup>×</sup>, V. S. Khrapai<sup>×, +1)</sup>*

<sup>×</sup>*Institute of Solid State Physics, Russian Academy of Sciences, 142432 Chernogolovka, Russia*

<sup>+</sup>*Moscow State University of Education, 29 Malaya Pirogovskaya Street, Moscow 119435, Russia*

<sup>\*</sup>*National Research University Higher School of Economics, 20 Myasnitskaya Street, Moscow 101000, Russia*

Submitted 9 декабря 2019 г.

We study the heat relaxation in current biased metallic films in the regime of strong electron-phonon coupling. A thermal gradient in the direction normal to the film is predicted, with a spatial temperature profile determined by the temperature-dependent heat conduction. In the case of strong phonon scattering the heat conduction occurs predominantly via the electronic system and the profile is parabolic. This regime leads to the linear dependence of the noise temperature as a function of voltage bias, in spite of the fact that all the dimensions of the film are large compared to the electron-phonon relaxation length. This is in stark contrast to the conventional scenario of relaxation limited by the electron-phonon scattering rate. A preliminary experimental study of a 200 nm thick NbN film indicates the relevance of our model for materials used in superconducting nanowire single-photon detectors.

Kinetics of the energy relaxation defines a temporal response of radiation detectors based on thin metallic films at low temperatures [1, 2, 3, 4, 5, 6]. According to advanced theoretical models [5, 7], the internal efficiency of the superconducting nanowire single-photon detectors (SNSPDs) depends critically on the time-scales of the electron-phonon (e-ph) relaxation  $\tau_{e-ph}$  and of the phonon escape in the substrate  $\tau_{esc}$ . Qualitatively, the  $\tau_{e-ph}$ , along with the diffusion coefficient of electrons, determines the characteristic size of the hot-spot mediated by the absorption of a photon, whereas the  $\tau_{esc}$ , if big enough, can limit the eventual relaxation time of the hot-spot [8, 9, 10]. In addition, important is the ratio of the electron and phonon heat capacities,  $C_e/C_{ph}$ , which defines the fraction of the photon energy going into the electron system [7, 11].

A correspondence of several microscopic time-scales and the relaxation time, usually probed in experiments on the amplitude modulated absorption of the radiation [12, 13, 14, 15], is not straightforward. The interpretation of such experiments invokes the models of the energy balance of varying complexity. In some cases, the inclusion of a specific relaxation bottleneck in the model [14, 15] can explain the relaxation times much longer than  $\tau_{e-ph}$ , in spite of a similar temperature dependence. The problem is even more intricate since the materials suitable for SNSPDs typically have  $C_e/C_{ph} \gtrsim 1$  near the superconducting transition temperature [7]. This, by the detailed balance, is equivalent to  $\tau_{e-ph} \gtrsim \tau_{ph-e}$ , where  $\tau_{ph-e}$  is the phonon re-absorption time by the electrons. The latter inequality is, essentially, the condition of the

strong coupling regime of the electron and phonon systems, which manifests in local thermal equilibration between them when  $\tau_{esc} \gg \tau_{ph-e}$ . In this regime, one would not expect the microscopic time-scales  $\tau_{e-ph}$  and  $\tau_{ph-e}$  to govern the relaxation process individually.

In this article we focus on the heat transport in a current biased disordered metallic film in the regime of strong coupling between the electrons and phonons. We investigate the thick film limit, in which the mean-free paths of both the electrons and phonons are small compared to the film thickness. In this case, the heat outflow in the substrate requires a thermal gradient transverse to the film, with the spatial profile determined by the temperature dependence of the total thermal conductivity. Remarkably, in a situation when the electron contribution to the heat conductivity dominates, the spatial profile is parabolic and insensitive to the parameters of the electron-phonon relaxation. Here, we predict a non-vanishing shot noise of the film with a Fano factor  $F = \sqrt{3}/2(d/l)$ , which is determined solely by the ratio of film thickness  $d$  and the length of the device  $l$ . Such a universal expression emphasizes the fact that the bottleneck for thermal relaxation in this case is imposed by the Wiedemann-Franz heat conduction transverse to the film, while the electron-phonon parameters drop out. Our preliminary measurements in a disordered 200 nm thick NbN film in the normal state are consistent with this result.

We consider a typical experiment on the heat relaxation in a metallic film on a substrate. The electric current  $I$  is biased through the film with thickness  $d$ , length  $l \gg d$ , width  $w \gg d$  and conductivity  $\sigma$  (see Fig. 1). The current distribution is uniform across the

<sup>1)</sup>e-mail: dick@issp.ac.ru

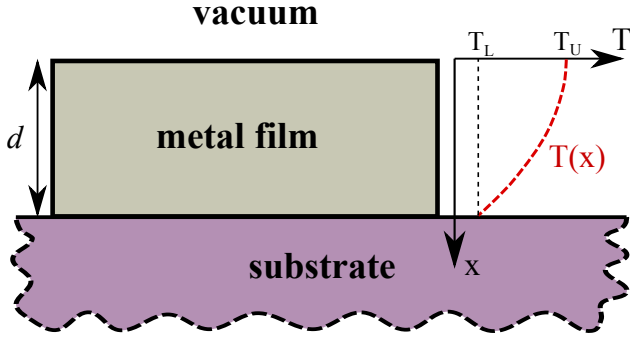


FIG. 1. The sketch of the experimental configuration under discussion. A conducting film with thickness  $d$  is located on a substrate and heated uniformly via Joule heat. Heat relaxation through the heat conduction to the substrate results in a temperature gradient transverse to the film in the direction  $x$ . The axes demonstrate parabolic temperature profile  $T(x)$  for the case of electron heat conduction according to Wiedemann-Franz law being dominant in the film. The  $(T_U)$  and  $(T_L)$  are the temperatures on the upper and lower surfaces, respectively.

film section so that the current density  $j = I/(wd)$ . For the experimentally preferred case of a film much longer than the electron-phonon relaxation length  $l_{e-ph} \ll l$ , we approximate the heat dissipation to occur entirely through the phonon conduction to the substrate. We also consider the case of strongly coupled electron and phonon subsystems, which allows us to define a single local equilibrium temperature  $T$ . This assumption requires the film thickness much larger than both electron-phonon and phonon-electron relaxation lengths  $l_{e-ph}, l_{ph-e} \ll d$ . As such, we neglect the in-plane  $T$  gradient and allow the temperature to be a function of a transverse coordinate  $x$  (see axes on fig. 1). We note that the temperature gradient between the upper and lower surfaces of the film is not addressed in most thermal relaxation studies, as it is either the electron-phonon coupling or the phonon thermal resistance at the interface that is considered to be the process limiting the heat transfer [14].

The regular thermal balance equation:

$$-\frac{\partial}{\partial x} \left( \kappa \frac{\partial}{\partial x} T \right) = \sigma^{-1} j^2, \quad (1)$$

sets the dissipation of Joule heat  $\sigma^{-1} j^2$  via combined electron and phonon thermal conductivity  $\kappa = \kappa_e + \kappa_{ph}$ . Obviously, the eq. (1) implies a transverse temperature gradient with a spatial profile determined by the

functional dependence  $\kappa(T)$ . Below we concentrate on a special case of negligible  $\kappa_{ph}$ , which is plausible in extremely disordered metallic films. Here, similar to amorphous materials [16], we expect the  $\kappa_{ph}$  to cut-off at increasing temperature owing to the Rayleigh scattering, which gives rise to a fast decay of the mean free path of the acoustic phonon  $l_{ph} \propto \omega^{-4}$  as a function of its frequency  $\omega$ . The electron thermal conductivity itself is given by the Wiedemann-Franz law  $\kappa_e = \mathcal{L} T \sigma$ , where  $\mathcal{L} = \pi^2 k_B^2 / 3e^2$  is the Lorenz number. This leads to the standard parabolic solution for  $T(x)$  [17]:

$$T^2(x) = T_L^2 + (T_U^2 - T_L^2) \left( 1 - \frac{x^2}{d^2} \right), \quad (2)$$

where temperatures at the upper and lower surfaces of the film are denoted as  $T_U \equiv T(x=0)$  and  $T_L \equiv T(x=d)$ , respectively. Note that here we took into account the boundary condition of zero heat flux on the upper surface, which is assumed to be placed in vacuum, see Fig. 1. The substitution of solution (2) into the equation (1) leads to the relation:

$$T_U^2 - T_L^2 = \frac{j^2 d^2}{\mathcal{L} \sigma^2}. \quad (3)$$

This solution satisfies the second boundary condition for the heat flux on the lower surface, namely that the heat flux density coincides with the Joule heat dissipated per unit area of the film.

As a next step, we presume, that the phonon escape into the bulk of the substrate provides an efficient path of heat relaxation in thin ( $\sim l_{ph-e}$ ) layer near the lower surface of the film, so that  $T_L \approx T_{bath}$ . Hence, considering the case of an intense heating  $T_U \gg T_{bath}$  we get the solution  $T_U = jd / \sigma \mathcal{L}^{1/2}$ .

The linear dependence  $T_U \propto I$  is reminiscent of the shot noise behavior in metallic diffusive conductors in the absence of electron-phonon relaxation [17, 18]. The same qualitative behaviour is the case for the noise temperature  $T_N$  of the whole sample. The  $T_N$  is determined by the average temperature, weighed by a local Joule power [19], which in present case corresponds to simple spatial averaging:

$$T_N = d^{-1} \int T(x) dx \approx \frac{\sqrt{3}}{4} \frac{e j d}{k_B \sigma} = \frac{\sqrt{3}}{4} \frac{d e V}{l k_B}, \quad (4)$$

where  $V = lI/dw\sigma$  is the applied voltage bias. Comparing the result (4) with the classical solution for a metallic diffusive conductor cooled via electron thermal conductivity through the contacts [17, 18]:  $T_N = \sqrt{3} e V / 2 k_B$ , we observe that the strong electron-phonon coupling leads to the drastic reduction of a

noise temperature by a geometrical factor  $2l/d \gg 1$ . Remarkably, while the suppression of the shot noise in the latter case is expected [20], the linear dependence  $T_N \propto V$  in the limit  $l, d, w \gg l_{e-ph}$  is special and manifests the relaxation bottleneck provided by the Wiedemann-Franz heat conduction transverse to the film. Finally, we give a rigorous expression for the  $T_N$ , valid for arbitrary relation between the  $T_U$  and  $T_L$  and obtained via integration of (2):

$$T_N = \frac{1}{2} \left( T_L + \frac{T_U^2}{\sqrt{T_U^2 - T_L^2}} \arccos \frac{T_L}{T_U} \right). \quad (5)$$

In the following we concentrate on a preliminary experimental study of thermal relaxation in a  $d = 200$  nm thick disordered NbN film. This material choice is natural for the purpose of reaching the regime of strong electron-phonon coupling. Much thinner NbN films of similar quality are routinely used in SNSPDs [11, 21] and characterized by  $\tau_{e-ph} \sim \tau_{ph-e} \sim 10$  ps near the superconducting transition temperature around  $T \approx 10$  K. This very well meets the above criterion  $l_{e-ph}, l_{ph-e} \ll d$ . The situation with phonon heat conductivity is more ambiguous [14], yet we expect the Rayleigh scattering of the acoustic phonons to become a limiting factor in this highly disordered material, at least at higher temperatures used in present experiment, such that  $\kappa_{ph} \ll \kappa_e$ .

The NbN film was grown the  $\text{SiO}_2$ -Si substrate at a room temperature using a DC magnetron sputtering system with 99.9999% pure niobium target. The preliminary vacuum was  $7 \cdot 10^{-7}$  Torr. During the deposition, the magnetron power was fixed at 200 W and the gas mixture ratio was  $\text{Ar} : \text{N}_2 = 40 : 7$ . In this way a strongly disordered NbN film was obtained with a room temperature resistivity of about  $800 \mu\Omega \cdot \text{cm}$  measured by a van der Pauw method. The NbN film was further patterned in a bridge of a width of  $w = 0.99 \mu\text{m}$  and a length of  $l = 27.5 \mu\text{m}$ . Prior to patterning, the metal Ti/Au (5 nm/200 nm) contact pads were fabricated with a lift-off method by means of electron-beam lithography and thermal evaporation. Next, a 250-nm thick protective Al mask was formed on the sample using the electron beam lithography and the electron beam evaporation. Finally, the film was etched in a mixture of Ar and  $\text{SF}_6$  gases and the aluminum mask removed in a KOH solution.

The experimental setup for noise thermometry was built in a homemade liquid  $^4\text{He}$  insert, with a tank circuit at a resonance frequency of 40 MHz at the input of a vapor-cooled high impedance low-noise amplifier ( $\approx 6$  dB gain and  $\approx 3 \times 10^{-27} \text{ A}^2/\text{Hz}$  input current

noise). The signal is further amplified by a chain of low-noise amplifiers at 300 K, filtered and measured via a power detector (see Supplemental Material of [22] for the details on shot-noise measurement technique and Ref. [23] for a recent review).

In this experiment, the voltage bias is applied to the NbN sample causing the Joule heating of the electron subsystem and the subsequent current noise increase. The noise temperature  $T_N$  is obtained from the Johnson-Nyquist relation  $S_I = 4k_B T_N / R$ .

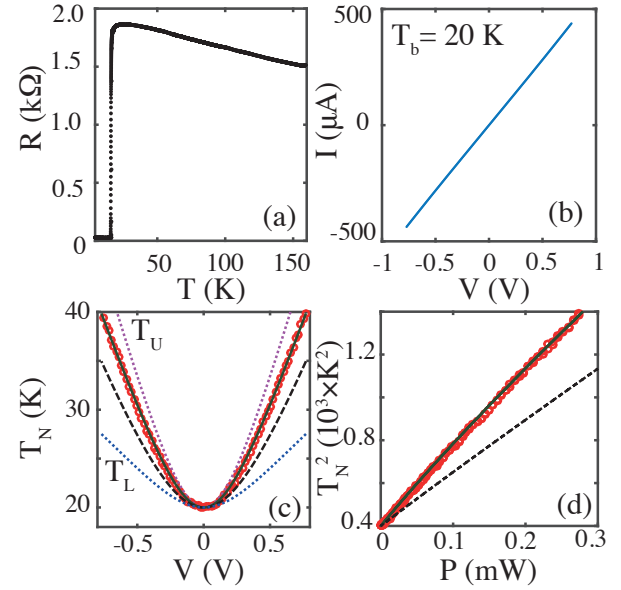


FIG. 2. The experimental data for 200-nm thick NbN sample. The sample goes to the superconducting state at 16 K, the width of the superconducting transition is about 2 K. (b) The I-V curve of the sample in the normal state at  $T_b = 20$  K. (c) The noise temperature  $T_N$  as a function of voltage bias  $V$ . The symbols are experimental data, the dashed line is the model result under the assumption of perfect thermal coupling between the film and the substrate and  $T_L = T_{\text{bath}}$ . The difference between the experiment and the model can be improved provided an additional relaxation bottleneck is taken into account in the form of Kapitza resistance (see text). The corresponding dependencies of  $T_N$  and  $T_L$ ,  $T_U$  are shown, respectively, by the solid line and two dotted lines. (d) The same data for the noise temperature as in (c) plotted as  $T_N^2$  in dependence of the Joule power  $P$ . The data supports the relevance of the Wiedemann-Franz bottleneck model for thermal relaxation (see text).

The panel Fig. 2a demonstrates the linear response resistance of the sample plotted as a function of the bath temperature. A superconducting transition occurs at  $T_C = 16$  K. On the panel Fig. 2b the I-V curve is

shown for  $T_{\text{bath}} = 20\text{ K}$  well above the  $T_C$ , which is linear up to 5% in all measurement range. These data demonstrate a conventional low-temperature transport response of our NbN sample.

The main experimental result is presented on the panel Fig. 2c. The symbols are experimental measurements, while the dashed line is the noise temperature according to the equations (3) and (5) with the corresponding  $l, d$  and  $T_L = T_{\text{bath}}$ . As expected, the noise temperature is low compared to the case of cooling via contacts (not shown), evidencing a strong thermal relaxation. At the same time, both the absolute value of the  $T_N$  and its functional dependence on the bias voltage  $V$  are close to our prediction. Fig. 2d presents the same data in the form of  $T_N^2$  as a function of the Joule power  $P$ , which also follows from our model. Again, we observe that the main heat relaxation bottleneck in this experiment is close to the one expected from the Wiedemann-Franz heat conduction transverse to the film.

The magnitude of the  $T_N$  growth with  $V$  is stronger in the experiment as compared to the model. We attribute this difference to the effect of an additional process weakly limiting the thermal relaxation in the film or in the substrate. In the following we demonstrate how one such possible mechanism, namely the Kapitza resistance owing to the acoustic mismatch between the film and the substrate, could explain the experimental data. In this scenario, the temperature at the lower surface of the film exceeds the bath temperature  $T_L > T_{\text{bath}}$  such that  $P/A = A_K(T_L^4 - T_{\text{bath}}^4)$ , where  $A = wl$  is the area covered by the film and  $A_K \sim 100 \div 1000 \text{ Wm}^{-2}\text{K}^{-4}$  is the parameter of the acoustic mismatch model [24]. Using the value of  $120 \text{ Wm}^{-2}\text{K}^{-4}$  we obtained the dependencies of the  $T_L$  and  $T_U$  on the bias voltage, which, via the eq. (5), closely describe the experimental dependence of the noise temperature  $T_N$ . In Fig. 2c these dependencies are shown, respectively, by the lower and upper dotted lines and by the solid line (the latter is also shown in Fig. 2d). In spite of a substantial increase of the  $T_L$  above the bath temperature, caused by the Kapitza resistance, a strong temperature gradient transverse to the film is the case. Still, we would like to stress that in order to draw a definite conclusion an independent measurement of the substrate-mediated relaxation bottleneck is necessary, which goes beyond the scope of this work.

In summary, we provide a model of thermal relaxation in disordered metallic films in the regime of strong electron-phonon coupling. We predict a sizeable temperature gradient transverse to the current-biased film, with a spatial profile determined by the heat

conduction of the material. In the limit of dominant heat conduction via electrons the temperature profile is parabolic and the noise temperature of the film scales linearly with the bias voltage. This resembles a universal shot noise behavior in diffusive conductors with negligible electron-phonon coupling, yet with the noise temperature drastically suppressed by the geometrical factor  $2l/d \gg 1$ . A preliminary experiment in a thick strongly disordered NbN film is not far from our model predictions.

We acknowledge valuable discussions with I.V. Tretyakov and A.V. Semenov. The theoretical model was developed with a support from the RFBR project 19-32-80037. The fabrication of the NbN sample and transport characterization were supported by the RSF project 17-72-30036. Noise measurements were performed with a support from the RSF project 19-12-00326. A.I.K. and E.M.B acknowledge financial support under the Grant of the President RF MK-1308.2019.2. The data analysis was performed within the state task of the ISSP RAS.

1. Chandra M Natarajan, Michael G Tanner, and Robert H Hadfield. Superconducting nanowire single-photon detectors: physics and applications. *Superconductor Science and Technology*, 25(6): 063001, apr 2012. doi: 10.1088/0953-2048/25/6/063001. URL <https://doi.org/10.1088/0953-2048/25/6/063001>.
2. Itamar Holzman and Yachin Ivry. Superconducting nanowires for single-photon detection: Progress, challenges, and opportunities. *Advanced Quantum Technologies*, 2(3-4):1800058, 2019. doi: 10.1002/qute.201800058. URL <https://onlinelibrary.wiley.com/doi/abs/10.1002/qute.201800058>.
3. F. Marsili, M. J. Stevens, A. Kozorezov, V. B. Verma, Colin Lambert, J. A. Stern, R. D. Horansky, S. Dyer, S. Duff, D. P. Pappas, A. E. Lita, M. D. Shaw, R. P. Mirin, and S. W. Nam. Hotspot relaxation dynamics in a current-carrying superconductor. *Phys. Rev. B*, 93: 094518, Mar 2016. doi: 10.1103/PhysRevB.93.094518. URL <https://link.aps.org/doi/10.1103/PhysRevB.93.094518>.
4. Lu Zhang, Lixing You, Xiaoyan Yang, Junjie Wu, Chaolin Lv, Qi Guo, Weijun Zhang, Hao Li, Wei Peng, Zhen Wang, and Xiaoming Xie. Hotspot relaxation time of NbN superconducting nanowire

- single-photon detectors on various substrates. *Scientific Reports*, 8(1):1486, 2018. ISSN 2045-2322. doi: 10.1038/s41598-018-20035-7. URL <https://doi.org/10.1038/s41598-018-20035-7>.
5. T. M. Klapwijk and A. V. Semenov. Engineering physics of superconducting hot-electron bolometer mixers. *IEEE Transactions on Terahertz Science and Technology*, 7(6):627–648, Nov 2017. doi: 10.1109/TTHZ.2017.2758267.
  6. I. Tamir, A. Benyamini, E. J. Telford, F. Gorniaczyk, A. Doron, T. Levinson, D. Wang, F. Gay, B. Sacépé, J. Hone, K. Watanabe, T. Taniguchi, C. R. Dean, A. N. Pasupathy, and D. Shahar. Sensitivity of the superconducting state in thin films. *Science Advances*, 5(3), 2019. doi: 10.1126/sciadv.aau3826. URL <https://advances.sciencemag.org/content/5/3/eaau3826>.
  7. D. Yu. Vodolazov. Single-photon detection by a dirty current-carrying superconducting strip based on the kinetic-equation approach. *Phys. Rev. Applied*, 7:034014, Mar 2017. doi: 10.1103/PhysRevApplied.7.034014. URL <https://link.aps.org/doi/10.1103/PhysRevApplied.7.034014>.
  8. Anthony J. Annunziata, Orlando Quaranta, Daniel F. Santavica, Alessandro Casaburi, Luigi Frunzio, Mikkel Ejrnaes, Michael J. Rooks, Roberto Cristiano, Sergio Pagano, Aviad Frydman, and Daniel E. Prober. Reset dynamics and latching in niobium superconducting nanowire single-photon detectors. *Journal of Applied Physics*, 108(8):084507, October 2010. doi: 10.1063/1.3498809. URL <https://doi.org/10.1063/1.3498809>.
  9. Francesco Marsili, Faraz Najafi, Charles Herder, and Karl K. Berggren. Electrothermal simulation of superconducting nanowire avalanche photodetectors. *Applied Physics Letters*, 98(9):093507, feb 2011. doi: 10.1063/1.3560458. URL <https://doi.org/10.1063/1.3560458>.
  10. Lu Zhang, Lixing You, Xiaoyan Yang, Yan Tang, Mengting Si, Kaixin Yan, Weijun Zhang, Hao Li, Hui Zhou, Wei Peng, and Zhen Wang. Hotspot relaxation time in disordered niobium nitride films. *Applied Physics Letters*, 115(13):132602, sep 2019. doi: 10.1063/1.5124335. URL <https://doi.org/10.1063/1.5124335>.
  11. E.M. Baeva, M.V. Sidorova, A.A. Korneev, K.V. Smirnov, A.V. Divochy, P.V. Morozov, P.I. Zolotov, Yu.B. Vakhtomin, A.V. Semenov, T.M. Klapwijk, V.S. Khrapai, and G.N. Goltsman. Thermal properties of NbN single-photon detectors. *Phys. Rev. Applied*, 10:064063, Dec 2018. doi: 10.1103/PhysRevApplied.10.064063. URL <https://link.aps.org/doi/10.1103/PhysRevApplied.10.064063>.
  12. D Rall, P Probst, M Hofherr, S Wünsch, K Il'in, U Lemmer, and M Siegel. Energy relaxation time in NbN and YBCO thin films under optical irradiation. *Journal of Physics: Conference Series*, 234(4):042029, jun 2010. doi: 10.1088/1742-6596/234/4/042029. URL <https://doi.org/10.1088/1742-6596/234/4/042029>.
  13. A. Kardakova, M. Finkel, D. Morozov, V. Kovalyuk, P. An, C. Dunscombe, M. Tarkhov, P. Mauskopf, T. M. Klapwijk, and G. Goltsman. The electron-phonon relaxation time in thin superconducting titanium nitride films. *Applied Physics Letters*, 103(25):252602, 2013. doi: 10.1063/1.4851235. URL <https://doi.org/10.1063/1.4851235>.
  14. Mariia V. Sidorova, A. G. Kozorezov, A. V. Semenov, Yu. P. Korneeva, M. Yu. Mikhailov, A. Yu. Devizenko, A. A. Korneev, G. M. Chulkova, and G. N. Goltsman. Nonbolometric bottleneck in electron-phonon relaxation in ultrathin wsi films. *Phys. Rev. B*, 97:184512, May 2018. doi: 10.1103/PhysRevB.97.184512. URL <https://link.aps.org/doi/10.1103/PhysRevB.97.184512>.
  15. Mariia Sidorova, Alexej Semenov, Heinz-Wilhelm Hübers, Konstantin Ilin, Michael Siegel, Ilya Charaev, Maria Moshkova, Natalia Kaurova, Gregory N. Goltsman, Xiaofu Zhang, and Andreas Schilling. Electron energy relaxation in disordered superconducting nbn films, 2019.
  16. R. C. Zeller and R. O. Pohl. Thermal conductivity and specific heat of noncrystalline solids. *Phys. Rev. B*, 4:2029–2041, Sep 1971. doi: 10.1103/PhysRevB.4.2029. URL <https://link.aps.org/doi/10.1103/PhysRevB.4.2029>.
  17. K. E. Nagaev. Influence of electron-electron scattering on shot noise in diffusive contacts. *Phys. Rev. B*, 52:4740–4743, Aug 1995. doi: 10.1103/PhysRevB.52.4740. URL <https://link.aps.org/doi/10.1103/PhysRevB.52.4740>.
  18. V. I. Kozub and A. M. Rudin. Shot noise in mesoscopic diffusive conductors in the limit of strong electron-electron scattering. *Phys. Rev. B*,

- 52:7853–7856, Sep 1995. doi: 10.1103/PhysRevB.52.7853. URL <https://link.aps.org/doi/10.1103/PhysRevB.52.7853>.
19. S. U. Piatrusha, V. S. Khrapai, Z. D. Kvon, N. N. Mikhailov, S. A. Dvoretzky, and E. S. Tikhonov. Edge states in lateral  $p - n$  junctions in inverted-band hgte quantum wells. *Phys. Rev. B*, 96: 245417, Dec 2017. doi: 10.1103/PhysRevB.96.245417. URL <https://link.aps.org/doi/10.1103/PhysRevB.96.245417>.
20. K.E. Nagaev. On the shot noise in dirty metal contacts. *Physics Letters A*, 169(1): 103 – 107, 1992. ISSN 0375-9601. doi: [https://doi.org/10.1016/0375-9601\(92\)90814-3](https://doi.org/10.1016/0375-9601(92)90814-3). URL <http://www.sciencedirect.com/science/article/pii/0375960192908143>.
21. Konstantin Smirnov, Alexander Divochiy, Yury Vakhtomin, Pavel Morozov, Philipp Zolotov, Andrey Antipov, and Vitaliy Seleznev. NbN single-photon detectors with saturated dependence of quantum efficiency. *Superconductor Science and Technology*, 31(3):035011, feb 2018. doi: 10.1088/1361-6668/aaa7aa. URL <https://doi.org/10.1088/2F1361-6668/2Faaa7aa>.
22. E. S. Tikhonov, M. Yu. Melnikov, D. V. Shovkun, L. Sorba, G. Biasiol, and V. S. Khrapai. Nonlinear transport and noise thermometry in quasiclassical ballistic point contacts. *Phys. Rev. B*, 90: 161405, Oct 2014. doi: 10.1103/PhysRevB.90.161405. URL <https://link.aps.org/doi/10.1103/PhysRevB.90.161405>.
23. S. U. Piatrusha, L. V. Ginzburg, E. S. Tikhonov, D. V. Shovkun, G. Koblmüller, A. V. Bubis, A. K. Grebenko, A. G. Nasibulin, and V. S. Khrapai. Noise insights into electronic transport. *JETP Letters*, 108(1):71–83, June 2018. doi: 10.1134/s0021364018130039. URL <https://doi.org/10.1134/s0021364018130039>.
24. Teemu Elo, Pasi Lähteenmäki, Dmitri Golubev, Alexander Savin, Konstantin Arutyunov, and Pertti Hakonen. Thermal relaxation in titanium nanowires: Signatures of inelastic electron-boundary scattering in heat transfer. *Journal of Low Temperature Physics*, 189(3-4):204–216, aug 2017. doi: 10.1007/s10909-017-1802-2. URL <https://doi.org/10.1007/s10909-017-1802-2>.